

Redoxactive Oligonucleotides: Synthesis and Properties of Flavocoenzyme-DNA

Alexandra Mees,^[a] Christoph Behrens,^[a] Anja Schwögler,^[a] Matthias Ober,^[a] and Thomas Carell*^[a]

Keywords: DNA / DNA damage / Flavin / Electron transfer / Oligonucleotides

The flavin heterocycle is the key component in the important and ubiquitous FMN and FAD coenzymes. As such, the flavin is able to catalyse oxygen-transfer reactions in many monooxygenases, as well as one- and two-electron transfer processes. We recently inserted the flavin heterocycle into oligonucleotides with the future goal of creating flavin-dependent ribozymes with redox-catalytic properties. We showed that a flavin inside duplex DNA is able to exchange electrons with its environment. These electron-exchange capabilities strongly modulate the fluorescence properties of the flavin heterocycle in DNA. Herein we report a detailed study of how DNA single and double strands change the

fluorescence intensity of the flavin cofactor. In agreement with the assumption that the flavin photooxidises predominately guanine and adenine bases, we observe the strongest fluorescence quenching when the flavin is in close contact with one of these purine nucleobases. No fluorescence quenching is observed in the presence of pyrimidine bases. We conclude that A and G in a DNA environment have a similar effect as Trp and Tyr in a protein surrounding, regarding the fluorescence properties of the flavin coenzyme.

(© Wiley-VCH Verlag GmbH & Co. KGaA, 69451 Weinheim, Germany, 2003)

Introduction

The incorporation of novel nucleotides into DNA is currently going through a renaissance. Major goals are: (1) the development of a third orthogonal, artificial DNA base pair, which can be enzymatically replicated in order to extend the genetic code,^[1–5] (2) the synthesis of metal-containing base pairs,^[6–9] and (3) the incorporation of catalytically competent nucleobases, which extend the catalytic repertoire of oligonucleotides.^[10,11] In this respect we hope that cofactor-modified DNA or RNA may, in the future, allow the direct in vitro selection of ribozymes with strongly extended catalytic properties.^[10,12–17] Flavins, are ubiquitous coenzymes that catalyse major biosynthetic reactions, including one- and two-electron transfer reactions and oxygen activation.^[18–20] Synthetic incorporation of a flavin coenzyme into oligonucleotides^[21–23] potentially combined with the powerful possibilities of the SELEX process^[24–26] may therefore, in the future, allow the direct evolution of redox-catalytic oligonucleotides.

Towards this goal we recently reported the preparation of a flavin coenzyme nucleobase, which can be incorporated into oligonucleotides by machine-assisted DNA/RNA synthesis.^[20,27,28] We also showed that the flavin coenzyme is redox-active in the oligonucleotide environment.^[29] The fla-

vin cofactor in its reduced state is, for example, able to transfer a single electron onto a UV-induced cyclobutane-pyrimidine dimer, inducing efficient repair of this otherwise mutagenic DNA lesion.^[30,31] Flavin-containing oligonucleotides gained in this respect self-healing properties.^[31]

Very recently Fontecave and co-workers noted, based on earlier studies of Yoneda et al.,^[32] a strong (sequence-independent!) reduction of the fluorescence intensity of a deazaflavin coenzyme at the end of oligonucleotides upon double-strand formation.^[21] This observation fueled the speculation that coenzyme nucleobases might allow the construction of novel oligonucleotide arrays (DNA chips).^[21]

The future development of redox-active oligonucleotides and of coenzyme-based DNA chips requires a detailed knowledge of how an oligonucleotide environment modulates the redox potentials and the fluorescence properties of redox coenzymes. Until today only the effect of a protein environment on the flavin fluorescence and its redox potential has been studied, for example with model compounds.^[33,34] Oligonucleotides, with their unique π -stacking and H-bonding arrangements, provide, however, a very different molecular setting, which we believe should strongly influence the optical and redox properties of an embedded flavin coenzyme due to the flat and fully conjugated heterocyclic character of the flavin molecule.

The fluorescence of the flavin coenzyme could be strongly influenced by nucleotides due to electron-transfer reactions, particularly, if the flavin is situated in the middle

^[a] Department of Chemistry, Philipps-Universität Marburg
Hans-Meerwein-Str., 35032 Marburg
Fax: (internat.) + 49-6421/2822189
E-mail: carell@staff.uni-marburg.de

of an oligonucleotide.^[35] Flavins in their oxidised redox state are known to be efficient type I photosensitizers and, as such, are able to photooxidise guanine and possibly also adenine bases.^[36] This property was recently exploited for the selective preparation of oxidative DNA lesions.^[37,38] Photoexcited reduced flavins are, in contrast, powerful electron donors and, as such, are able to reduce all nucleobases.^[39,40]

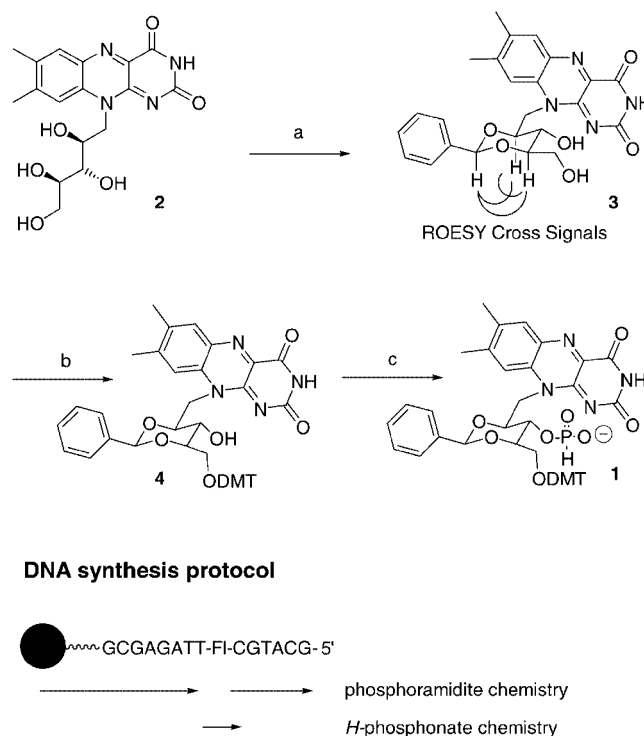
Results and Discussion

Synthesis and Molecular Modelling

We recently reported a synthetic strategy that allows the replacement of any given nucleobase in a DNA strand by a flavin coenzyme.^[20,31] Herein we report a systematic investigation of the fluorescence properties of the incorporated flavin. The study revealed the interesting fact that the flavin fluorescence is, in contrast to what has been observed by the Fontecave group for the deazaflavin, strongly sequence-dependent.

Scheme 1 shows the synthesis of the flavin building block **1** (via the compounds **2**, **3**, and **4**) as recently reported^[20] and depicts schematically the solid-phase scheme for the incorporation of **1** into DNA. Table 1 contains a list of the prepared DNA strands **5–16**, into which the flavin coenzyme was inserted, together with the calculated and found molecular masses of the flavin-DNA strands and the measured melting points in the case of double strands. The structure of **3** was confirmed by a ROESY experiment, which revealed the indicated correlations (Scheme 1). The solid-phase procedure developed for the incorporation of

the flavin *H*-phosphonate into DNA was also described recently.^[20] It requires a combination of phosphoramidite and *H*-phosphonate chemistry.^[29,41–43] The sequence in the 3'-direction to the flavin is prepared by standard phosphoramidite



Scheme 1. Synthesis of the flavin *H*-phosphonate **1** and depiction of the solid-phase protocol: a: PhCH(OMe)₂, CSA, DMF, 14%; b: DMTCl, pyridine, 77%; c: PCl₃, 1,2,4-triazole, *N*-methylmorpholine, 81%

Table 1. Sequences of the DNA strands **5–16** and their calculated and found molecular masses; melting temperatures of the double strands **9–16** ($c_{\text{DNA}} = 3 \times 10^{-6}$ M DNA, 150 mM NaCl, 10 mM Tris buffer, pH = 7.4) determined at 260 nm; F = Flavin

		Mol. mass (calcd.)	Mol. mass ^[a] (found)	Melting temp. ^[b] T_m [°C]
5	5'-GCGCATFTTACGCG-3'	4474.8	4475.0	
6	5'-GCGCATFATACGCG-3'	4483.8	4484.0	
7	5'-GCGCAFGTTACGCG-3'	4499.8	4499.9	
8	5'-GCGCAAFTTACGCG-3'	4483.8	4484.0	
9	5'-GCGCAATTTACGCG-3'	4261.8	4261.5	60
	3'-CGCGTTAAATGCGC-5'	4261.8	4261.7	
10	5'-GCGCAAFTTACGCG-3'	4483.8	4484.0	45
	3'-CGCGTTAAATGCGC-5'	4261.8	4261.7	
11	5'-GCGCAAFTTACGCG-3'	4483.8	4484.0	43
	3'-CGCGTTTAAATGCGC-5'	4252.7	4254.1	
12	5'-GCGCAAFTTACGCG-3'	4483.8	4484.0	42
	3'-CGCGTTGAATGCGC-5'	4277.8	4277.8	
13	5'-GCGCAAFTTACGCG-3'	4483.8	4484.0	40
	3'-CGCGTTCAATGCGC-5'	4237.7	4236.9	
14	5'-GCGCATFTTACGCG-3'	4474.8	4475.0	44
	3'-CGCGTATAATGCGC-5'	4261.8	4262.9	
15	5'-GCGCATFATACGCG-3'	4483.8	4484.0	43
	3'-CGCGTATTATGCGC-5'	4292.8	4294.0	
16	5'-GCGCAFGTTACGCG-3'	4499.8	4499.9	53
	3'-CGCGTTCAATGCGC-5'	4277.8	4279.1	

^[a] Determined by MALDI-TOF mass spectrometry (matrix: 2,4,6-trihydroxyacetophenone). ^[b] For the exact conditions see Exp. Sect.

idite chemistry. The flavin itself is coupled as an *H*-phosphonate. The DNA segment in the 5'-direction to the flavin is then continued using phosphoramidite chemistry.

Figure 1 shows two calculated DNA double strands that contain the flavin nucleobase inside the duplexes. The modelling results support our view that the flavin heterocycle stacks inside the double helix structure (see below). The benzylidene protecting group, however, interferes with the stacking of the flavin in the 5'-direction. Double strands were calculated, which feature either a pyrimidine base (T, Figure 1, b) or a purine base (A, Figure 1, a) 5' to the flavin base. Both nucleobases are strongly destacked in our modelling, indicating that the π -stacking interaction of the flavin base is strongly reduced in the 5'-direction. In both cases, however, the stacking is almost perfect in the 3'-direc-

tion. In this direction, the flavin stacks both on top of a thymine base, as shown in Figure 1 (a), or on top of an adenine base as shown in Figure 1 (b). This result is very interesting in connection with the herein reported fluorescence study, because it allowed us to investigate the modulation of the flavin fluorescence not only by the kind of nucleobase close to the flavin but also by the stacking situation.^[44]

Fluorescence Studies with Flavin-Containing DNA Single Strands

The Effect of the Base Sequence

In order to evaluate how strongly different nucleobases influence the flavin fluorescence we first studied the fluor-

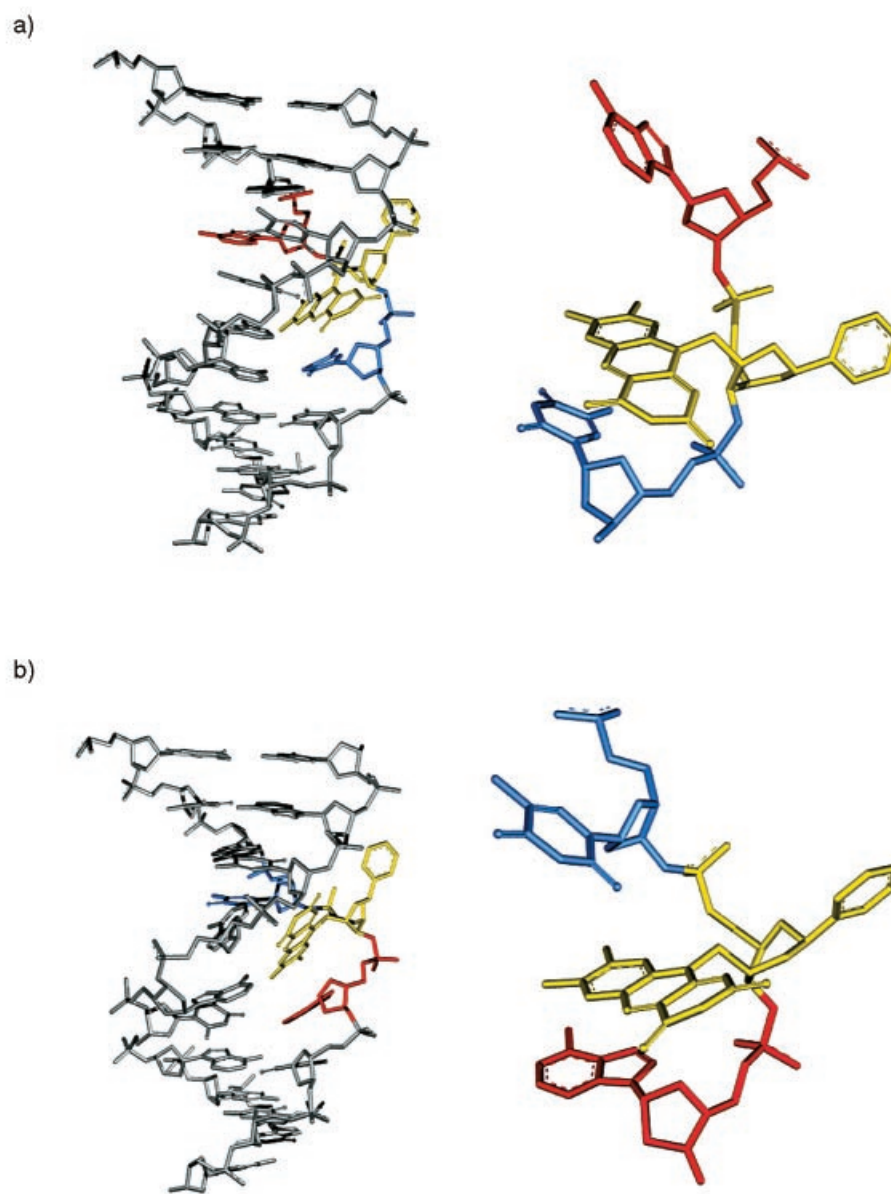


Figure 1. Molecular modelling of the flavin building block **1** inside a typical DNA double strand in water (for details see Exp. Sect.); sequence: a) 5'-AFT-3', b) 5'-TFA-3'

escence of the flavin in the four single strands **5–8**. The measured fluorescence spectra are depicted in Figure 2. Strong coenzyme fluorescence is observed if the flavin is flanked by two thymines (strand **5**). We observe a strong fluorescence decrease if 3'-T is replaced by an adenine as in strand **6**. Replacement of 5'-T by A, as in strand **8**, gives almost no fluorescence quenching, showing that the unfavourable stacking towards the 5'-end exists also in the DNA single strand. Even stronger fluorescence reduction is observed with a guanine placed 3' to the flavin fluorophore. The increasing fluorescence quenching from T through A to G in the 3'-direction is in line with the decrease of the oxidation potentials ($E_{\text{OX,T}} = 1.9 \text{ V}$, $E_{\text{OX,A}} = 1.7 \text{ V}$, $E_{\text{OX,G}} = 1.24 \text{ V}$).^[45,46] The fluorescence quenching of the flavin in the presence of an A and a G is observed for the first time and reflects, in our opinion, the efficient photooxidation of both nucleobases by the flavin chromophore.^[47,48] This photooxidation, we believe, is caused by an electron-transfer reaction between the purines G and A and the photoexcited flavin. Such an electron transfer is strongly distance-dependent and is therefore influenced by the stacking situation in a DNA duplex.^[49] In order to investigate this effect in more detail, we prepared the double strands **11** and **14–16** and studied how the two purine nucleobases in the 3'- and 5'-direction influence the fluorescence of the flavin. The next section describes the general (determined with the duplexes **10–13**) characteristics of flavin-containing DNA double strands followed by a systematic evaluation of how the base sequence and the counterbase influence the flavin fluorescence intensity.

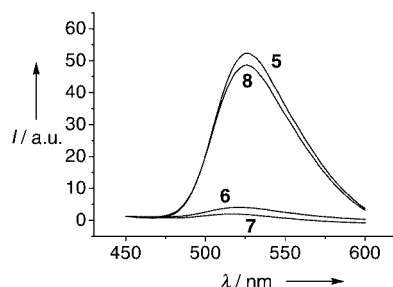


Figure 2. Steady-state fluorescence spectra of the flavin-containing DNA single strands **5–8** ($c_{\text{DNA}} = 3 \times 10^{-6} \text{ M}$ in 0.01 M Tris buffer, 150 mM NaCl, $\text{pH} = 7.4$, $\lambda_{\text{ex.}} = 360 \text{ nm}$, $\lambda_{\text{em.}} = 520 \text{ nm}$, room temp.)

Investigation of Flavin-Containing DNA Double Strands

General Characteristics of Flavin-Containing DNA Double Strands

The flavin heterocycle possesses, in principle, the same H-bonding capabilities as the natural base thymine. We therefore investigated first the potential pairing properties of the flavin in a DNA duplex. To this end UV-melting curves of double strands containing the flavin-base in contact with the four canonical bases as counterbases were measured. A

typical UV-melting curve is depicted in Figure 3 (a).^[50] Table 1 contains a list of the determined melting temperatures. In Figure 3 (a), both a heating and a cooling curve are shown. It is clearly evident that the flavin-containing DNA double strands feature a typical, reversible melting behaviour. No hysteresis is observed. Figure 3 (a) depicts a melting curve measured at 260 nm , where all the DNA bases absorb. Figure 3 (b) shows the same melting curve measured at 460 nm . This is a wavelength at which only the flavin molecule is able to absorb light. Both obtained melting points (T_m) are, within the error limit, identical, indicating that the flavin is situated inside the helix and that it destacks upon duplex melting in a cooperative manner similar to the other nucleobases.

In comparison to the undisturbed double strand **9** with a T:A base pair ($T_m = 60 \text{ }^\circ\text{C}$) we observe a rather strong decrease of the melting temperature ($T_m = 45 \text{ }^\circ\text{C}$) after replacement of one of the thymines by flavin **1** in duplex **10**. This melting point is similar to a T_m value of a typical mismatch. For example, the double strand with a T:T mismatch melts at approximately the same temperature (data not shown). Even lower melting points were noted for the Fl:G(**12**), Fl:C(**13**) and Fl:T(**11**) “base pairs” indicating that in the Fl:A situation some of the destabilisation induced by the flavin in the duplex is compensated by a small stabilising effect, maybe by hydrogen bonding of the flavin to the adenine.

Most interesting are the fluorescence melting curves, one of which is depicted in Figure 4. Curve (a) shows the fluorescence behaviour of the flavin **1** in the DNA single strand **8**. The fluorescence of the flavin decreases steadily with increasing temperature, possibly due to the promotion of flavin bending modes, which accelerate the internal conversion process. The corresponding flavin-containing DNA double strand **11**, however, shows a very different fluorescence behaviour with increasing temperature (Figure 4, curve b). We observe a strong fluorescence increase at the melting temperature. After complete melting, the temperature-dependent fluorescence decrease continues. These measurements underline that the flavin fluorescence is strongly quenched within the DNA duplex environment.

The CD curves of all flavin-containing double strands are very typical for an overall B-form double strand. Figure 5 shows as an example the spectrum measured for the double strand **11**. The maxima at 280 and 220 nm and the minimum at 250 nm indicate overall B conformation of the flavin-containing duplexes. Based on the CD spectra, and fluorescence data, together with our modelling results, we propose that the flavin disrupts the duplex only in its close vicinity, predominately towards the 5'-direction. The overall B-duplex structure remains, however, intact.

The Effect of the Base Sequence on the Fluorescence of the Flavin in DNA Double Strands

In the four DNA double strands **11** and **14–16**, a thymine was always chosen as the flavin counterbase. The flavin is, however, in all these double strands incorporated into

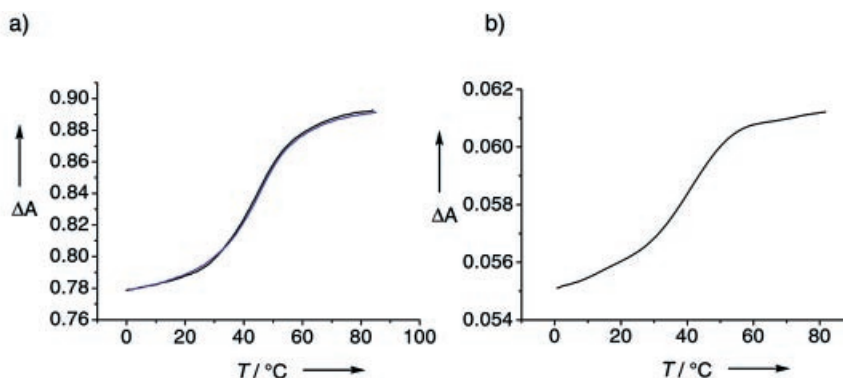


Figure 3. UV melting curves: a) measured at 260 nm and b) measured at 460 nm ($c_{\text{DNA}} = 3 \times 10^{-6}$ M in 0.01 M Tris buffer, 150 mM NaCl, pH = 7.4, temperature gradient 0.5 °C/min)

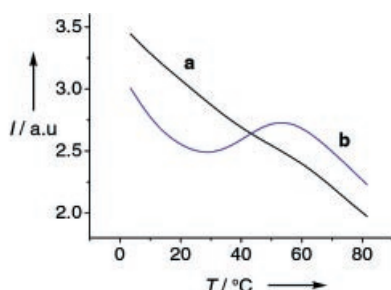


Figure 4. Typical fluorescence melting curve of a flavin-containing DNA single strand measured with **8** (a) and of a flavin-containing double strand measured with **11** (b) ($c_{\text{DNA}} = 3 \times 10^{-6}$ M in 0.01 M Tris buffer, 150 mM NaCl, pH = 7.4, $\lambda_{\text{ex.}} = 360$ nm, $\lambda_{\text{em.}} = 520$ nm, temperature gradient 2.5 °C/min)

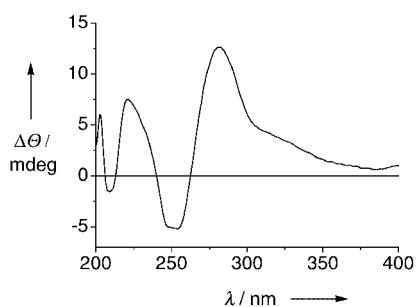


Figure 5. CD spectrum of the flavin-containing DNA double strand **11** (averaged from 10 independent measurements, $c_{\text{DNA}} = 3 \times 10^{-6}$ M in 0.01 M Tris buffer, 150 mM NaCl, pH = 7.4)

a different base sequence. The measured fluorescence spectra are depicted in Figure 6. In general, the observed data are very similar to those obtained for the single strands **5–8**. Strong coenzyme fluorescence is observed if the flavin is flanked by two thymines (strand **14**). We observe a strong fluorescence decrease if the 3'-T is replaced by an adenine, as in the double strand **15**. Again, a stronger fluorescence reduction is observed with a guanine placed on the 3'-side of the flavin fluorophore (strand **16**). Switching the adenine from the 3'-side of the flavin (double strand **15**) to the 5'-side (double strand **11**) again gives rise to strong fluorescence. This result underlines the fact that the fluorescence

reduction of the flavin base is induced exclusively by a purine in the 3'-position. These fluorescence data strongly support, therefore, our idea that the fluorescence reduction is caused by an electron-transfer phenomenon. In the investigated double strands, the flavin is in a similar structural context. We can therefore exclude that the fluorescence reduction is influenced by a different shielding of the flavin from water.

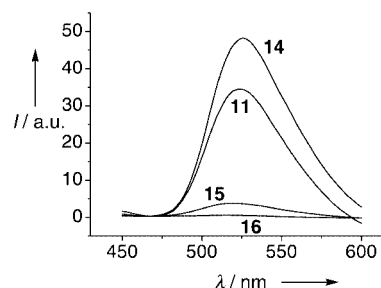


Figure 6. Steady state fluorescence spectra of the flavin-containing DNA double strands **11**, **14–16** ($c_{\text{DNA}} = 3 \times 10^{-6}$ M in 0.01 M Tris buffer, 150 mM NaCl, pH = 7.4, $\lambda_{\text{ex.}} = 360$ nm, $\lambda_{\text{em.}} = 520$ nm, room temp.)

The Effect of the Counterbase on the Fluorescence of the Flavin in DNA Double Strands

In order to evaluate if the rather strong fluorescence modulation can be exploited to monitor the kind of nucleobase opposite the flavin in a DNA double strand, we ana-

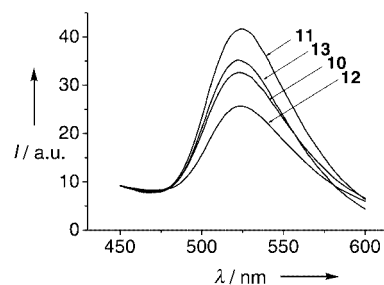


Figure 7. Fluorescence spectra of the DNA double strands **10–13** ($c_{\text{DNA}} = 3 \times 10^{-6}$ M in 0.01 M Tris buffer, 150 mM NaCl, pH = 7.4, $\lambda_{\text{ex.}} = 360$ nm, $\lambda_{\text{em.}} = 520$ nm)

lyzed the fluorescence of the four double strands **10–13**. They contain the flavin **1** in the same sequence context but it faces each of the four nucleobases as the counterbase. The obtained fluorescence spectra are shown overlaid in Figure 7. In general, the modulation of the fluorescence intensity is small. We observe, however, a clear influence by the counterbase: the highest fluorescence is observed with a T or C counterbase (**11** and **13**), intermediate fluorescence is measured with an A counterbase (**10**) and the strongest fluorescence decrease is observed with the G counterbase (**12**).

Conclusion

The incorporation of coenzymes like flavins and deazaflavins into oligonucleotides is desired for the construction of catalytic DNA/RNA with properties that extend into the domain of redox catalysis. The fluorescence properties of these coenzymes in an oligonucleotide environment is a very critical property because it is influenced by electron-transfer reactions with the nucleobases. This, in turn, strongly affects the photo-oxidising and photo-reducing capabilities of such catalytically competent nucleobases embedded within oligonucleotides.

We find that the fluorescence intensity of a flavin molecule inside a DNA duplex is a very complex property. The fluorescence intensity is first of all influenced by the sequence and hence by the kind of neighbouring nucleobase. The fluorescence in single and double strands is high in a pure pyrimidine environment and reduced in the presence of a guanine and even of an adenine, which reflects the photooxidising properties of the flavin heterocycle. In agreement with the fact that the guanine base is most easily oxidised, we observe the strongest fluorescence reduction in the presence of this base.

The fluorescence intensity is furthermore reduced upon duplex formation, which packs the flavin inside the π -stacked double-strand environment as evident from the fluorescence melting curve. Additional, but smaller, modulation of the fluorescence signal originates from the counterbase. Again, guanine was found to quench most efficiently followed by adenine. None, or only very small, fluorescence quenching is observed if pyrimidine bases are present as counterbases.

Efficient π -stacking is another factor that modulates the fluorescence properties of the flavin. In our system the flavin is well stacked in the 3'-direction and badly stacked towards 5'. A purine base reduces the flavin fluorescence only if it is positioned 3' to the flavin showing that the basis of the fluorescence reduction is a strong distance-dependent process, probably an electron-transfer reaction.

The complex flavin fluorescence behaviour in DNA reported here seems to reduce the chance for flavins to function as efficient probes in the standard DNA array technology. However, the coenzyme is surprisingly useful for the precise monitoring of the nucleobase environment in its vicinity. This could be exploited for the detection of single

nucleotide polymorphisms (SNPs). Whether the modulation of the fluorescence intensity in the steady state is strong enough to compete with, for example, signals obtainable from molecular beacons, is questionable. To us, it seems, however, possible to monitor the environment using time-resolved fluorescence spectroscopy. Investigations in this direction are under way.

This report presents the first study of the fluorescence property of a flavin coenzyme in DNA. The described results will be the basis for all attempts to create flavin-DNA-based chips or the evolution of redox-active oligonucleotides using the SELEX approach.

Experimental Section

General Methods: UV/Vis spectra: Varian Bio 100 spectrophotometer at room temperature; λ_{max} in nm (ϵ in $\text{M}^{-1}\text{cm}^{-1}$). Melting points were measured using a Cary Bio 100 (Varian) with a Cary temperature controller and a sample transport accessory with a multi cell block. Temperature gradient $0.5\text{ }^{\circ}\text{C}/\text{min}$. Oligonucleotides were dissolved in a Tris buffer (10 mM Tris, 150 mM NaCl, pH = 7.4). CD spectra were recorded using a JASCO J-810 at $20\text{ }^{\circ}\text{C}$. Fluorescence spectra were measured using a JASCO FP750 fluorimeter equipped with a single monochromator with $\pm 5\text{ nm}$, 150 Hg/Xe lamp, in 1-cm quartz cuvettes at $15\text{ }^{\circ}\text{C}$. Mass spectra were recorded with a Bruker Biflex MALDI-TOF mass spectrometer (Matrix: 2,4,6-trihydroxyacetophenone, 0.5 M in H_2O /diammonium citrate/ 0.1 M in H_2O). Oligonucleotide synthesis was performed with an Expedite 8900 Gene synthesiser. Pac-amidites were purchased from Glen Research. Controlled pore glass bead support was purchased from Applied Biosystems. Acetonitrile for the oligonucleotide synthesis was obtained from Roth. All solvents were stored for 12 h over 4 \AA molecular sieves prior to oligonucleotide synthesis. HPLC was performed with a Merck-Hitachi Lachrome HPLC system with a flow of $1\text{ mL}/\text{min}$ using Nucleosil RP18 ($250\text{ mm} \times 4\text{ mm}$, $100\text{ \AA}/5\text{ }\mu\text{m}$ or $250\text{ mm} \times 4\text{ mm}$, $120\text{ \AA}/3\text{ }\mu\text{m}$) columns from Macherey–Nagel. HPLC-grade solvents were purchased from Fluka. All oligonucleotides were detected at 260 nm . For analytical oligonucleotide HPLC a linear gradient was used. Preparative HPLC was performed with a Nucleosil RP C18 column ($250\text{ mm} \times 21\text{ mm}$, $100\text{ \AA}/5\text{ }\mu\text{m}$). Solvent system: A = 0.1 M NEt_3/HOAc in H_2O , B = 0.1 M NEt_3/HOAc in $\text{H}_2\text{O}/\text{MeCN}$ (1:4). Molecular modelling was performed with Tripos Sybyl V6.8. The structures were dissolved in a droplet of water containing 1500 explicit water molecules. A simulated annealing run (1000 fs, 700 K; relaxation for 2500 fs to 50 K) was executed using the force field mmff94s. The structure with the smallest potential energy was finally minimised using the Powell iteration method.

10-[(2S,4S,5S,6R)-5-Hydroxy-6-(hydroxymethyl)-2-phenyl-1,3-dioxan-4-yl]methyl-7,8-dimethylbenzo[g]pteridine-2,4(3H,10H)-dione (3**):** Riboflavin **2** (5.0 g, 13 mmol), $\text{PhCH}(\text{OMe})_2$ (2.00 g, 13 mmol) and CSA (0.60 g, 2.6 mmol) were suspended in DMF (200 mL) and allowed to react at $50\text{ }^{\circ}\text{C}$ and 60 mbar for 16 h. DMF was removed at $50\text{ }^{\circ}\text{C}$ and 12 mbar, then under high vacuum. The suspension was filtered, the residual material was washed with CHCl_3 ($3 \times 100\text{ mL}$). The filtrate was washed with water ($3 \times 200\text{ mL}$) and with saturated NaHCO_3 solution (200 mL). After chromatographic purification ($\text{CHCl}_3/\text{MeOH}$, 30:1, then 20:1), 0.83 g (0.179 mmol, 14%) product **3** was isolated. M.p. $218\text{--}220\text{ }^{\circ}\text{C}$ (decomp.). R_f (silica gel; $\text{CH}_2\text{Cl}_2/\text{MeOH}$, 20:1) = 0.28. IR (KBr): $\tilde{\nu} = 3146, 2940, 1718, 1654, 1579, 1544, 1085, 1020\text{ cm}^{-1}$.

^1H NMR (500 MHz, pyridine): δ = 2.18, 2.31 (2 s, 6 H, 2 CH_3), 4.28–4.30 (m, 2 H, 3',4'-H), 4.35–4.37, 4.50–4.58 (2 m, 2 H, 5'-H), 4.70–4.78 (m, 1 H, 2'-H), 5.19–5.38, 5.68–5.80 (2 m, 2 H, 1'-H₂), 5.85 (s, 1 H, $\text{CH}_{\text{benzylidene}}$), 6.44–6.92 (m, 1 H, 5'-OH), 7.30–7.38, 7.56–7.57 (2 m, 5 H, $\text{CH}_{\text{arom.}}$), 7.87 (s, 1 H, 6-H), 8.14 (s, 1 H, 9-H), 8.73 (s, 1 H, NH), 13.43 (s, 1 H, 3'-OH) ppm. ^{13}C NMR (125 MHz, pyridine): δ = 19.00, 20.80, 47.77, 62.12, 64.85, 80.40, 83.58, 100.90, 118.63, 126.92 (2 C), 128.34 (2 C), 129.07, 131.76, 132.91, 134.99, 136.15, 138.03, 138.87, 146.21, 151.67, 156.83, 161.02 ppm. FAB-MS (positive; 3-NOBA): m/z = 465 (100) $[\text{MH}]^+$. HRMS (FAB⁺): calcd. $\text{C}_{24}\text{H}_{25}\text{N}_4\text{O}_6$ (464.1774 $[\text{MH}]^+$); found 465.1776.

10-[(2S,4S,5S,6R)-6-[Bis(4-methoxyphenyl)(phenyl)methoxy]methyl-5-hydroxy-2-phenyl-1,3-dioxan-4-yl)methyl]-7,8-dimethylbenzo[g]pteridine-2,4(3H,10H)-dione (4): A suspension of pyridine (40 mL) and **3** (0.60 g, 1.29 mmol) was stirred for 1 h with molecular sieves under nitrogen. After addition of dimethoxytrityl chloride (0.74 g, 2.20 mmol), the suspension was stirred at room temperature for 3 h. Then methanol (5 mL) was added and the solvents were evaporated to dryness. The material was further dried under high vacuum. After chromatographic purification ($\text{CHCl}_3/\text{MeOH}/\text{NEt}_3$, 30:1:0.2), 0.76 g (0.99 mmol, 77%) of **4** was isolated. M.p. 179–180 °C, R_f (silica gel; $\text{CHCl}_3/\text{MeOH}$, 20:1) = 0.4. IR (KBr): $\tilde{\nu}$ = 3471, 3180, 2920, 1654, 1544, 1400, 1086, 1030 cm^{-1} . ^1H NMR (500 MHz, CDCl_3): δ = 2.40, 2.43 (2 s, 6 H, 2 CH_3), 3.77 (s, 6 H, PhOCH_3), 3.37–3.40, 3.48–3.50, 3.95–3.98, 4.23–4.29, 4.90–5.01 (5 m, 7 H, 1',2',3',4',5'-H), 5.64 (s, 1 H, $\text{CH}_{\text{benzylidene}}$), 6.76–6.78, 7.15–7.42 (2 m, 18 H, $\text{CH}_{\text{arom.}}$), 7.92, 8.04 (2 s, 2 H, 6,9-H), 8.56 (s, 1 H, NH), 8.63 (s, 1 H, OH) ppm. ^{13}C NMR (125 MHz, CDCl_3): δ = 19.47, 21.29, 47.50, 55.17 (2 C), 63.77, 68.15, 80.06, 80.57, 86.04, 100.47, 113.06 (4 C), 118.11, 123.73, 125.93, 126.71, 127.72, 128.01, 128.15, 128.79, 128.87, 130.09, 130.14, 130.86, 132.28 (2 C), 132.31 (2 C), 135.34, 135.39, 135.95, 136.02, 137.35, 137.56, 144.95, 148.25, 149.83, 150.76, 154.08, 158.42, 159.10 ppm. FAB-MS (positive; 3-NOBA): m/z = 766 (20) $[\text{M}^+]$, 303 (100) $[\text{DMTr}^+]$. HRMS (FAB⁺): calcd. $\text{C}_{45}\text{H}_{43}\text{N}_4\text{O}_8$ 766.3002 $[\text{M}^+]$; found 766.2999 $[\text{M}^+]$.

(2S,4R,5S,6S)-4-[Bis(4-methoxyphenyl)(phenyl)methoxy]methyl-6-[7,8-dimethyl-2,4-dioxo-3,4-dihydrobenzo[g]pteridin-10(2H)-yl]-methyl-2-phenyl-1,3-dioxan-5-yl Hydrogen phosphonate (1): Under nitrogen a solution of PCl_3 (2 mol/L in CH_2Cl_2 , 0.64 mL, 1.28 mmol) was diluted with CH_2Cl_2 (10 mL). *N*-Methylmorpholine (405 mg, 4.00 mmol) and 1,2,4-triazole (277 mg, 4.00 mmol) were then added. The suspension was stirred at room temperature for 30 min and finally cooled to 0 °C. A solution of **4** (200 mg, 0.26 mmol) in CH_2Cl_2 (5 mL) was added dropwise. After 30 min at 0 °C, buffer $[(\text{HNEt}_3)\text{HCO}_3]$, pH = 7.8, 1 mL, 5 mL] was added. After 30 min of hydrolysis, the emulsion was extracted with CH_2Cl_2 (100 mL) and buffer (100 mL). The *H*-phosphonate **1** was finally purified by flash chromatography ($\text{CHCl}_3/\text{MeOH}/\text{NEt}_3$, 15:1:0.2, then 10:1:0.2 then 8:1:0.2). Evaporation of the solvent in vacuo yielded 199 mg of **1** (0.21 mmol, 81%) as a yellow powder. M.p. 162–163 °C, R_f (silica gel; $\text{CHCl}_3/\text{MeOH}/\text{NEt}_3$, 15:1:0.1) = 0.18. IR (KBr): $\tilde{\nu}$ = 3420, 3139, 1654, 1545, 1400, 1086, 1050, 1030 cm^{-1} . ^1H NMR (300 MHz, CDCl_3): δ = 1.31 [t, J = 7.5 Hz, 9 H, $(\text{CH}_3\text{CH}_2)_3\text{N}$], 2.43, 2.45 (2 s, 6 H, 2 \times CH_3), 3.13 [q, J = 7 Hz, 6 H, $(\text{CH}_3\text{CH}_2)_3\text{N}$], 3.37 (dd, J = 3.1 Hz, 10.3, 1 H, 5'-H), 3.53–3.56 (m, 1 H, 5'-H), 3.77, 3.78 (2 s, 6 H, PhOCH_3), 3.92–3.96, 4.39–4.55, 4.86–4.94, 5.76–5.80 (4 m, 5 H, 1',2',3',4'-H), 5.43 (s, 1 H, CH), 7.26 (d, J_{PH} = 632 Hz, 1 H, PH), 6.76–6.84, 7.09–7.61 (2 m, 18 H, $\text{CH}_{\text{arom.}}$), 7.91, 8.00 (2 s, 2 H, 6,9-H) ppm. ^{31}P NMR (121 MHz, CDCl_3): δ = 4.21 (dd, J = 630.11, PH) ppm. ESI-MS (MeOH , negative): m/z = 829 (50) $[\text{M}^-]$, 527 (100).

Oligonucleotide Synthesis: Oligonucleotide synthesis was performed with an Expedite 8900 DNA Synthesiser, controlled by an IBM-compatible PC. Synthesis of the oligonucleotides was performed by using a modified 1.0 μmol cycle and Pac-amidites. Solvents and solutions were prepared according to the manufacturer's protocol. The phosphoramidite (0.1 M in MeCN) and 1*H*-tetrazole (0.5 M in MeCN) solutions were equal in concentration to those used for the synthesis of natural oligodeoxynucleotides. Average coupling yields monitored by on-line trityl assay were generally in the range of 95–99%. All syntheses were run in the trityl-off mode. The concentrations used for *H*-phosphonate chemistry were 0.13 M in MeCN/pyridine (1:1) for the *H*-phosphonate and 0.17 M in MeCN/pyridine for the activator adamantoylcarbonyl chloride, respectively. The cartridge was washed with MeCN/pyridine (1:1) prior to the coupling. The coupling time was 10–15 min. Capping, oxidation and detritylation were the same as for standard phosphoramidite chemistry. After DNA synthesis we pumped first a solution prepared of 0.1 M I_2 in MeCN H_2O with *N*-methylmorpholine as the base, than a solution containing 0.1 M I_2 in MeCN H_2O with NEt_3 through the cartridge to obtain full oxidation of the *H*-phosphonate to the phosphate.

DNA Purification: For the deprotection and purification of the oligonucleotides, the solid support was suspended in 25% NH_3 in $\text{H}_2\text{O}/\text{EtOH}$ (3:1; 1 mL) and shaken at 20 °C for 16 h in an Eppendorf thermo shaker to achieve deprotection and cleavage of the oligonucleotide from the CPG material. The solution was filtered, concentrated and the residue was suspended in H_2O . The DNA was purified by HPLC (C_{18} -RP, 0–40% B in 30 min, A = 0.1 M triethylammonium acetate in H_2O , B = 0.1 M triethylammonium acetate in $\text{H}_2\text{O}/80\%$ MeCN.) DNA-containing fractions were concentrated to dryness and redissolved in H_2O .

Acknowledgments

The work was supported by the Volkswagen Stiftung, the Fonds of the Chemische Industrie, the Deutsche Forschungsgemeinschaft and the Ministry of Education and Research (BMBF: Neue Medien in der Bildung). We thank two unknown referees for their valuable comments.

- [1] J. A. Piccirilli, T. Krauch, S. E. Moroney, S. A. Benner, *Nature* **1990**, *343*, 33–37.
- [2] C. Y. Switzer, S. E. Moroney, S. A. Benner, *Biochemistry* **1993**, *32*, 10489–10496.
- [3] D. L. McMinn, A. K. Ogawa, Y. Wu, J. Liu, P. G. Schultz, F. E. Romesberg, *J. Am. Chem. Soc.* **1999**, *121*, 11585–11586.
- [4] E. L. Tae, Y. Wu, G. Xia, P. G. Schultz, F. E. Romesberg, *J. Am. Chem. Soc.* **2001**, *123*, 7439–7440.
- [5] Y. Wu, A. K. Ogawa, M. Berger, D. L. McMinn, P. G. Schultz, F. E. Romesberg, *J. Am. Chem. Soc.* **2000**, *122*, 7621–7632.
- [6] H. Weizman, Y. Tor, *J. Am. Chem. Soc.* **2001**, *123*, 3375–3376.
- [7] K. Tanaka, A. Tengeji, T. Kato, N. Toyama, M. Shiro, M. Shionoya, *J. Am. Chem. Soc.* **2002**, *124*, 12494–12498.
- [8] N. Zimmermann, E. Meggers, P. G. Schultz, *J. Am. Chem. Soc.* **2002**, *124*, 13684–13685.
- [9] S. Atwell, E. Meggers, G. Spraggon, P. G. Schultz, *J. Am. Chem. Soc.* **2001**, *123*, 12364–12367.
- [10] O. Thum, S. Jäger, M. Famulok, *Angew. Chem. Int. Ed.* **2001**, *40*, 3990–3991.
- [11] K. Sakthivel, C. F. Barbas III, *Angew. Chem. Int. Ed.* **1998**, *37*, 2872–2875.
- [12] P. Burgstaller, M. Famulok, *J. Am. Chem. Soc.* **1997**, *119*, 1137–1138.
- [13] P. Burgstaller, T. Hermann, C. Huber, M. Famulok, *Nucleic Acids Res.* **1997**, *25*, 4018–4027.

- [14] C. Huber, P. Burgstaller, M. Famulok, *Nucleosides Nucleotides* **1997**, *16*, 717–720.
- [15] M. A. W. Eaton, D. W. Hutchinson, *Biochim. Biophys.* **1973**, *319*, 218–387.
- [16] T. M. Tarasow, S. L. Tarasow, B. E. Eaton, *Nature* **1997**, *389*, 54–57.
- [17] T. W. Wiegand, R. C. Janssen, B. E. Eaton, *Chem. Biol.* **1997**, *4*.
- [18] C. Walsh, *Acc. Chem. Res.* **1980**, *13*, 148–155.
- [19] T. C. Bruice, *Acc. Chem. Res.* **1980**, *13*, 256–262.
- [20] A. Schwögler, T. Carell, *Org. Lett.* **2000**, *2*, 1415–1418.
- [21] C. Dueymes, J. L. Decout, P. Peltie, M. Fontecave, *Angew. Chem. Int. Ed.* **2002**, *41*, 486–489.
- [22] C. Frier, J.-L. Decout, M. Fontecave, *J. Org. Chem.* **1997**, *62*, 3520.
- [23] C. Frier, J.-F. Mouscadet, J.-L. Decout, C. Auclair, M. Fontecave, *Chem. Commun.* **1998**, 2457–2458.
- [24] A. A. Beaudry, G. F. Joyce, *Science* **1992**, *257*, 635–641.
- [25] G. F. Joyce, *Curr. Biol.* **1996**, *6*, 965–967.
- [26] L. Gold, *J. Biol. Chem.* **1995**, *270*, 13581–13584.
- [27] A. Schwögler, V. Gramlich, T. Carell, *Helv. Chim. Acta* **2000**, *83*, 2452–2463.
- [28] K. Berlin, R. K. Jain, M. D. Simon, C. Richert, *J. Org. Chem.* **1998**, *63*, 1527–1535.
- [29] C. Behrens, M. Ober, T. Carell, *Eur. J. Org. Chem.* **2002**, 3281–3289.
- [30] C. Behrens, L. T. Burgdorf, A. Schwögler, T. Carell, *Angew. Chem. Int. Ed.* **2002**, *114*, 1841–1844.
- [31] A. Schwögler, L. T. Burgdorf, T. Carell, *Angew. Chem. Int. Ed.* **2000**, *39*, 3918–3920.
- [32] Y. Nakamura, T. Akiyama, Y. Yoneda, K. Tanaka, F. Yoneda, *Chem. Pharm. Bull.* **1993**, *41*, 778–780.
- [33] E. C. Breinlinger, C. J. Keenan, V. M. Rotello, *J. Am. Chem. Soc.* **1998**, *120*, 8606–8609.
- [34] A. Niemz, V. M. Rotello, *Acc. Chem. Res.* **1999**, *32*, 44–52.
- [35] I. Girault, J.-L. Ravanat, C. Frier, M. Fontecave, J. Cadet, J.-L. Decout, *Nucleosides Nucleotides* **1999**, *18*, 1345–1347.
- [36] K. Ito, S. Inoue, K. Yamamoto, S. Kawanishi, *J. Biol. Chem.* **1993**, *268*, 13221–13227.
- [37] H. Ikeda, I. Saito, *J. Am. Chem. Soc.* **1999**, *121*, 10836–10837.
- [38] K. Kino, I. Saito, H. Sugiyama, *J. Am. Chem. Soc.* **1998**, *120*, 7373–7374.
- [39] M. P. Scannel, D. J. Fenick, S.-R. Yeh, D. E. Falvey, *J. Am. Chem. Soc.* **1997**, *119*, 1971–1977.
- [40] S.-R. Yeh, D. E. Falvey, *J. Am. Chem. Soc.* **1992**, *114*, 7313–7314.
- [41] J.-C. Bologna, F. Morvan, J.-L. Imbach, *Eur. J. Org. Chem.* **1999**, 2353–2358.
- [42] A. P. Guzaev, M. Manoharan, *J. Org. Chem.* **2001**, *66*, 1798–1804.
- [43] P. M. Jung, G. Histan, R. L. Letsinger, *Nucleosides Nucleotides* **1994**, *13*, 1597–1605.
- [44] B. Giese, S. Wessely, *Chem. Commun.* **2001**, 2108–2109.
- [45] S. Steenken, S. V. Jovanovic, *J. Am. Chem. Soc.* **1997**, *119*, 617–618.
- [46] C. A. M. Seidel, A. Schulz, M. H. M. Sauer, *J. Phys. Chem.* **1996**, *100*, 5541–5553.
- [47] C. Lu, W. Lin, W. Wang, Z. Han, S. Yao, N. Lin, *Phys. Chem. Chem. Phys.* **2000**, *2*, 329–334.
- [48] B. Giese, J. Amaudrut, A.-K. Köhler, M. Spormann, S. Wessely, *Nature* **2001**, *4112*, 318–320.
- [49] J. Jortner, M. Bixon, T. Langenbacher, M. E. Michel-Beyerle, *Proc. Natl. Acad. Sci. U. S. A.* **1998**, *95*, 12759–12765.
- [50] K. J. Breslauer, in *Methods in Enzymology*, vol. 259 (“Energetics of Biological Macromolecules”) (Eds.: M. L. Johnson, G. K. Ackers), **1995**, p. 221–242.

Received February 5, 2003